FROM THE RADIATION PHYSICS DEPARTMENT (DIRECTOR: ASSOC. PROF. H. SKÖLDBORN), SAHLGRENSKA SJUKHUSET, UNIVERSITY OF GOTHENBURG, S-413 45 GOTHENBURG, SWEDEN.

DUAL PHOTON ABSORPTIOMETRY IN LUMBAR VERTEBRAE

II. Precision and reproducibility

B. O. ROOS

Details of the experimental technique for the determination of the bone mineral content in a lumbar vertebra have been described previously (ROOS et coll. 1970, ROOS & SKÖLDBORN 1974). The method involves the use of two isotopes which emit gamma radiation with different energies (^{241}Am with 59.6 keV and ^{137}Cs with 662 keV). The radiation sources are so arranged that their gamma radiation passes the object to be measured in a common collimated radiation beam (Fig. 1). The transmitted gamma radiation is registered digitally with a scintillation detector—both photon energies simultaneously. The measurement is performed during a pre-set period of time at a number of points along a path transversally (x-direction) over the patient. The measuring path is projected over the centre of a selected vertebra (usually L3). Application of the law of exponential attenuation enables calculation of the amount of bone mineral (g cm^{-2}) at each point along the measuring path, irrespective of the amount of soft tissue. The bone mineral values are plotted as a function of position thus giving a bone profile curve which may be integrated over a base line between end-points on either side of the vertebra. The resulting area is termed A and is proportional to the bone mineral content in the unit g cm^{-1}.

Submitted for publication 2 August 1974.

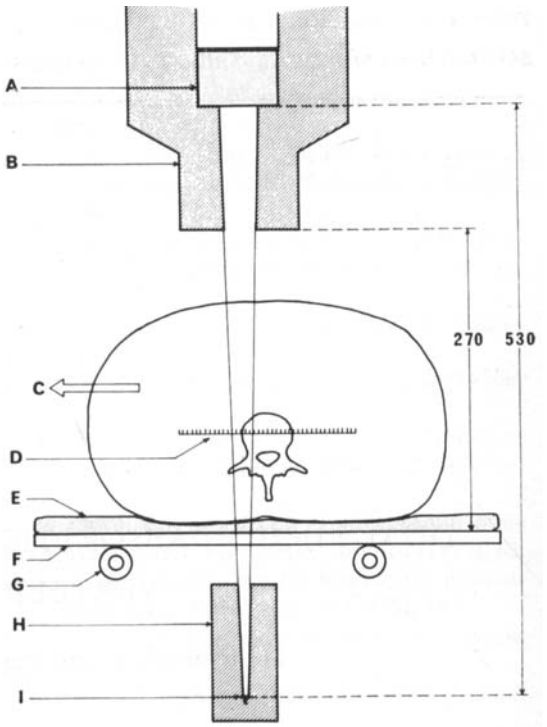

Fig. 1. Diagram showing measuring procedure. A = scintillation crystal, B = lead collimator for the detector, C = patient's direction of movement, D = scale for demonstrating the successive measuring positions, E = polythene mattress, F = couch, G = ball bearing, H = source container with collimation of emitted radiation beam, I = radiation sources. Distances stated in mm.

The photon flux which meets the scintillation crystal depends upon radiation geometry, thickness and structure of the object being measured, and the activity of the radiation sources. The distance between the radiation sources and the scintillation crystal is 530 mm. The beam is collimated so that the cross-sectional area is rectangular At a height of 90 mm above the couch (Fig. 1) it has an effective size of 14 mm × 25 mm with the long side parallel to the couch. In measurements in patients the radiation beam passes the trunk in the p.a. direction at the level of the third lumbar vertebra. A large individual variation exists, which has a considerable influence on the attenuation of the radiation especially the low energy part from ^{241}Am.

The ^{137}Cs source has an activity of 5 mCi and an effective diameter of 3 mm. The ^{241}Am source is flat and circular with an activity of 100 mCi and an active diameter of 7.2 mm. Due to self-absorption, the source must be relatively thin (0.7 mm) and if higher activity is required the diameter must also be increased, which was not desirable with the measuring geometry chosen. The flux of low energy photons to the scintillation crystal is thus also limited by the physical properties of the radiation source.

The random nature of the radiation decay means that the number of counts obtained will vary according to the Poisson distribution. This results in a mathematically well-defined precision in the final result—the area A.

Repeated measurements in the same individual give varying values of A. The scatter of these values is called the total precision, which consists of variations caused by the decay and subject variations. "Subject variations" include all factors which cannot be reproduced exactly from one measurement to another, for example adjustment variations, movements of the subject during the measurement or variations in the position of the subject.

Theory for the influence of the poisson scatter on A

Fundamental statistical concepts. The standard deviation of a variable x, which is assumed to be normally distributed, is estimated using the following formula:

$$s = \sqrt{\frac{\sum(x-\bar{x})^2}{n-1}} \tag{1}$$

where

x = the individual measurement values,
$\bar{x}$ = the mean value of the measurement values,
n = number of determinations of x.

The coefficient of variation V represents the standard deviation in per cent of the mean value:

$$V = 100\frac{s}{\bar{x}} \tag{2}$$

For the Poisson distribution, the standard deviation of the distribution is equal to the root of the true mean value. For a value y, included in a Poisson distribution, the standard deviation σ is thus estimated according to the following:

$$\sigma = \sqrt{y} \tag{3}$$

If z is a function of the variables $y_1, y_2, \ldots y_n$, the standard deviation of z is estimated as follows:

$$\sigma = \sqrt{\sum_{i=1}^{n}\left(\frac{\partial z}{\partial y_i}\right)^2 \cdot \sigma_{y_i}^2} \tag{4}$$

When comparing two independent series of measurements with the mean values $\bar{x}_1$ and $\bar{x}_2$ Student's t test is used for testing the significance of difference between the mean values. If each measurement series comprises n measurements, the standard deviation for the difference is

$$s_{diff} = \sqrt{\frac{s_1^2 + s_2^2}{n}} \tag{5}$$

and the confidence interval is

$$(\bar{x}_2 - \bar{x}_1) - t \cdot s_{diff}, (\bar{x}_2 - \bar{x}_1) + t \cdot s_{diff} \quad (6)$$

For example, if $n = 10$ and the confidence level is 95 %, $t = 2.262$.

Formalism of the method. Theoretical deductions (ROOS & SKÖLDBORN 1974) have shown that the result of a stationary measurement may be expressed as

$$m_B = \frac{N - D_{SF} m_F}{D_{SB}} \quad (7)$$

where

m_B = the bone mineral mass in the path of the radiation beam (g cm^{-2})
m_F = adipose tissue mass in the path of the beam (g cm^{-2})
D_{SF} and D_{SB} = terms comprising mass attenuation coefficients only.

Further,

$$N = -\mu'_S \ln (R - kR') + \mu_S \ln R' + C \quad (8)$$

where

μ'_S = the mass attenuation coefficient (cm^2 g^{-1}) for 662 keV (^{137}Cs) in lean soft tissue
μ_S = the mass attenuation coefficient (cm^2 g^{-1}) for 59.6 keV (^{241}Am) in lean soft tissue
R' = number of counts in the ^{137}Cs channel
R = number of counts in the ^{241}Am channel
k = the fraction of R' registered in the ^{241}Am channel due to Compton scattering
C = a constant

N is calculated according to equation (8) for each measurement point and plotted as a function of the position x (Fig. 2). Integration between the points x_1 and x_n gives the area A, which in practice is summed according to the following:

$$A = \left[\sum_{i=2}^{n-1} N_i - \frac{n-2}{2} (N_1 + N_n) \right] \cdot \Delta x \quad (9)$$

If the summation limits x_1 and x_n are chosen so that the radiation beam passes outside the vertebra, the values N_1 and N_n will represent the soft tissue on either side of the vertebra. The summation includes values which exceeds the straight base line, connecting N_1 and N_n. The area A divided by the constant D_{SB} gives the bone mineral content (g cm^{-1}) in a transverse section through the vertebra. From here on the results of the measurements will be presented as the relative quantity A.

The standard deviation of N and A. In the expression for N, equation (8), the two variables, the number of counts R and R', are Poisson distributed. Differentiation and application of equation (3) gives

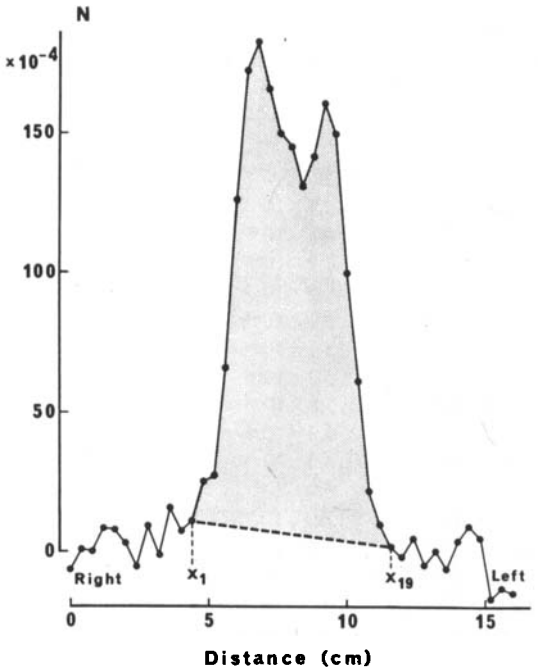

Fig. 2. Bone profile showing N as a function of measuring position x for normal subject ML, measurement No. 4.

$$\frac{\partial N}{\partial R} = -\frac{\mu_S'}{R - kR'}$$

$$\frac{\partial N}{\partial R'} = \frac{\mu_S}{R'} + \frac{k\mu_S'}{R - kR'}$$

$$\sigma_R = \sqrt{R}$$

$$\sigma_{R'} = \sqrt{R'}$$

Insertion in equation (4) gives the standard deviation for N:

$$\sigma_N = \sqrt{\left(\frac{\mu_S'}{R - kR'}\right)^2 \cdot R + \left(\frac{\mu_S}{R'} + \frac{k\mu_S'}{R - kR'}\right)^2 \cdot R'} \tag{10}$$

Equation (10) thus gives the standard deviation for the individual variables N_1, N_2, ..., N_n. By applying equation (4) the standard deviation of the area A may be calculated as follows:

$$\sigma_A = \sqrt{\left[\sum_{1=2}^{n-1} \sigma_{N_1}^2 + \left(\frac{n-2}{2}\right)^2 (\sigma_{N_1}^2 + \sigma_{N_n}^2)\right] \cdot (\Delta x)^2} \tag{11}$$

Numerical example. As an example, measurement no. 4 in the normal subject ML is taken from the measurement series presented below. Fig. 2 presents the resulting polygon (N) as a function of the measurement position x for this example. The

Table 1

Measurement results and standard deviation for the normal person ML, measurement no. 4. Measurement time 0.5 min per point, $\Delta x = 0.4$ cm

Position	R	R′	N	σ_N
x_1	230 844	172 265	10.7×10^{-4}	4.9×10^{-4}
x_2	240 097	176 650	25.2×10^{-4}	4.8×10^{-4}
x_3	233 592	174 776	28.2×10^{-4}	4.9×10^{-4}
x_4	212 866	171 070	65.9×10^{-4}	4.9×10^{-4}
x_5	191 121	168 283	125.9×10^{-4}	5.0×10^{-4}
x_6	177 982	167 069	172.6×10^{-4}	5.1×10^{-4}
x_7	179 683	168 709	183.1×10^{-4}	5.0×10^{-4}
x_8	188 505	170 838	166.2×10^{-4}	5.0×10^{-4}
x_9	194 905	171 924	149.9×10^{-4}	5.0×10^{-4}
x_{10}	200 838	173 807	145.2×10^{-4}	4.9×10^{-4}
x_{11}	200 719	172 434	130.7×10^{-4}	5.0×10^{-4}
x_{12}	195 537	171 431	141.7×10^{-4}	5.0×10^{-4}
x_{13}	186 919	169 732	161.0×10^{-4}	5.0×10^{-4}
x_{14}	191 254	170 477	149.9×10^{-4}	5.0×10^{-4}
x_{15}	219 873	176 698	100.0×10^{-4}	4.9×10^{-4}
x_{16}	254 799	184 871	61.4×10^{-4}	4.7×10^{-4}
x_{17}	273 260	186 755	21.8×10^{-4}	4.7×10^{-4}
x_{18}	275 272	186 170	9.7×10^{-4}	4.7×10^{-4}
x_{19}	300 693	192 806	1.8×10^{-4}	4.6×10^{-4}

end-points chosen as the summation limits are designated x_1 and x_{19} (Fig. 2). The number of counts recorded and the corresponding values for N and σ_N obtained from equations (8) and (10) are given in Table 1. For the calculations the following experimentally determined values of the mass attenuation coefficients and the factor of Compton contribution, k, have been used (Roos 1970):

$$\mu_S = 0.1867 \quad \text{cm}^2\,\text{g}^{-1}$$
$$\mu_S' = 0.0814 \quad \text{cm}^2\,\text{g}^{-1}$$
$$k = 0.045$$

By means of equations (9) and (11)

$$A = 692.7 \times 10^{-4}$$
$$\sigma_A = 24.2 \times 10^{-4}$$
$$V_A = 100\frac{\sigma_A}{A} = 3.5\,\%$$

is calculated.

According to equation (11) the measurement points $x_2 \ldots x_{18}$ contribute equally to the coefficient of variation (3.5 %) while the contributions of the end points

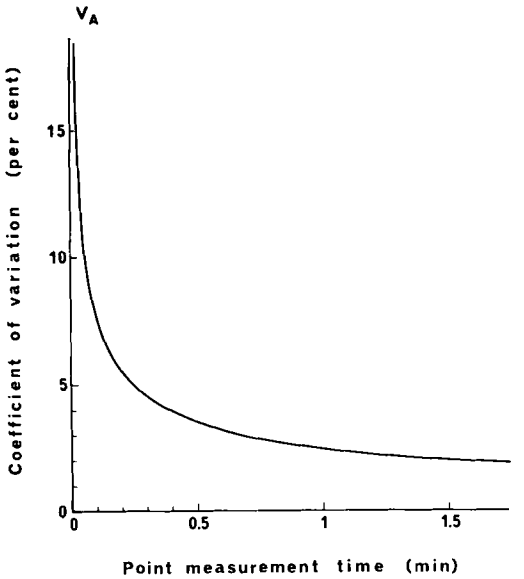

Fig. 3. Coefficient of variation V_A as a function of measuring time t for normal person ML, measurement No. 4.

(x_1 and x_{19}) are weighted with the factor $((n-2)/2^2)$, which in this case will be 72.25. Differentiation of equation (11) and insertion of the numerical values from Table 1 (x_{10}) shows that in the differential of σ_A in this case the end points contribute 89 per cent and intermediate points 11 per cent. The positioning of the base-line thus has a great influence on the precision. This problem is discussed further below.

σ_N is dependent upon the mass attenuation coefficients and the number of counts. Partial differentiation of equation (10) with respect to R and R′ and insertion of the numerical values for a measurement point (x_{10} in Table 1) gives the following result:

$$\frac{\partial \sigma_N}{\partial R} = -2.15 \times 10^{-10}$$

$$\frac{\partial \sigma_N}{\partial R'} = -11.17 \times 10^{-10}$$

σ_N thus shows 5 times greater dependence on R′, which represents the higher photon energy. In order to improve the precision with the given photon energies the activity of ^{137}Cs may therefore be increased. The influence of the mass attenuation coefficients has been analysed by WOOTEN (1971). His results show that in dichromatic measurements through a tissue thickness of 1.2 cm bone plus 20 cm soft tissue the lower photon energy should be in the range 35 to 40 keV and the higher should exceed 200 keV in order to give maximum precision of the bone mineral measurement. However, WOOTEN used different and optimal measuring times for the two photon energies, while the method using simultaneous measurement requires the same measuring times. The results of WOOTEN are thus not applicable in detail in the present investigation.

Table 2

Sex, age, height and weight of four normal subjects

Case	Sex	Age	Height (cm)	Weight (kg)
1	m	22	187	84
2	m	35	180	78
3	f	48	157	54
4	f	24	160	57

The influence of the measuring time. The precision of N, σ_N, is inversely proportional to the root of the measuring time t. This is deducted from equation (10). Let R_1, R_1' and $\sigma_{N,1}$ represent measured number of counts and the standard deviation at the measuring time 1 min per point. With another measuring time, t min per point, the number of counts will be $t \cdot R_1$ and $t \cdot R_1'$, respectively. Insertion of these number of counts in equation (10) gives $\sigma_N = \sigma_{N,1}/\sqrt{t}$ and insertion of these σ_N in equation (11) gives $\sigma_A = \sigma_{A,1}/\sqrt{t}$. Fig. 3 illustrates the coefficient of variation V_A as a function of the measuring time t for the example shown in Table 1. The coefficient of variation increases rapidly with decreasing time of measuring. With the present source activities we have chosen to measure each point 0.5 min.

Reproducibility

The reproducibility of the method including both decay and subject variation has been investigated by repeated measurements in 4 normal subjects. The standard deviation of the results was compared with the theoretical standard deviation according to counting statistics.

The sex, age, height and weight of the four normal subjects are given in Table 2. The measurements in the normal subjects were performed during a period of 12 days. A maximum of one measurement per day was performed except for subject SS who was once measured in the morning and in the afternoon on the same day.

Measuring conditions. The electrical equipment was powered throughout the period of measurement. Adjustment of the spectrum was performed routinely both in the morning and in the afternoon. The stability was good and only small changes of the positions and widths of the channels were necessary. No permanent drifting in the electronics could be demonstrated. Each measurement was performed using the following routine:

Measurement with the subjects lying on their backs with cushions under their knees in order to achieve stability with the lumbar region horizontal,
Fluoroscopy and focusing the central beam through the centre of L3,
Distance between measurement points, $\Delta x = 0.4$ cm,
Measuring time $t = 0.5$ min at each point.

Table 3

Results of measurements in four normal subjects. A_{mean} = mean value of 10 measurements, s_A = standard deviation of these measurements and $\sigma_{A,mean}$ = mean value of σ_A for each subject (x 10^{-4}). Figures within brackets after each standard deviation represent the corresponding coefficient of variation

	Case			
	1	2	3	4
A_{mean}	822.7	631.3	660.2	672.2
s_A	41.2 (5.0 %)	35.9 (5.7 %)	22.3 (3.4 %)	24.1 (3.6 %)
$\sigma_{A,mean}$	29.2 (3.6 %)	30.5 (4.8 %)	23.7 (3.6 %)	23.2 (3.5 %)

Data Processing. The primary data consisted of the number of counts R and R′ for each measurement point. After completion of the measurement these data were processed as follows:

Calculation of N and σ_N according to equations (8) and (10),
Plotting of N as a function of the position x (Fig. 2),
Measurement of the width at half maximum of the curve and, knowing the width of the radiation beam (14 mm), localization of the end points (x_1 and x_n) which are definitely located outside the vertebra,
Calculation of A and σ_A according to equations (9) and (11),
Calculation of the mean value of A and the standard deviation s_A according to equation (1),
Calculation of the mean value of σ_A for each normal person.
The results for the four normal persons appear in Table 3.

Long-term precision

The stability of the apparatus during a prolonged period of time was checked with 5 cm wide aluminium discs measured in a water phantom. Discs of two different thicknesses were used, Al 1 and Al 2. The results of the measurement series, each comprising 10 measurements appear in Table 4.

For the aluminium disc Al 1 the change in A_{mean} was -17.4×10^{-4} (2.2 %). The standard deviation of this change, s_{diff}, was 10.8×10^{-4} and the corresponding confidence interval at the 95 % level was (-41.9×10^{-4}, $+7.1 \times 10^{-4}$). Theoretically the standard deviation of the change, σ_{diff}, was 8.5×10^{-4} with a 95 % confidence interval of (-34.1×10^{-4}, -0.7×10^{-4}). The three measurement series of Al 2 gave a mean value of 560.1×10^{-4}.

Discussion

The standard deviation of N, σ_N, is partly due to the relationship between the registered number of counts R and R′. It has previously been demonstrated that the

Table 4

Results of five series of measurements of aluminium discs, each series comprising 10 measurements. A_{mean} = mean value of measurements in each series, s_A = standard deviation for each series and $\sigma_{A,mean}$ = mean value of σ_A for each series, (x 10^{-4}). Figures within brackets after each standard deviation represent the corresponding coefficient of variation

	Al 1		Al 2		
	June 1972	Jan. 1974	Jan. 1974	April 1974	June 1974
A_{mean}	803.5	786.1	561.9	556.9	561.4
s_A	32.0 (4.0 %)	12.3 (1.6 %)	6.8 (1.2 %)	8.6 (1.6 %)	12.5 (2.2 %)
$\sigma_{A,mean}$	17.8 (2.2 %)	20.3 (2.6 %)	15.5 (2.8 %)	14.9 (2.7 %)	14.9 (2.7 %)

precision is improved if the number of counts of the higher photon energy is increased at the expense of the lower energy. Fig. 4 shows σ_N as a function of R providing $R + R' = 374645$ (measuring point x_{10} in Table 1). The curve is limited by the asymptotes A, where $R = k\ R'$, and D, where $R' = 0$. C represents the number of counts for the particular measuring point and B the minimum of the curve where $\sigma_N = 4.6 \times 10^{-4}$. This minimum would have been reached if the activity of the ^{241}Am source had been reduced from 100 to 70 mCi and the activity of the ^{137}Cs source had been increased from 5 to 7 mCi. It should be observed that the result is valid for this example only. A somewhat fatter patient would permit a relatively lesser transmission of the lower photon energy and thus a value of σ_N closer to the optimum. If the thickness of the subject is increased further there is a risk of arriving on the ascending leg of the curve between A and B, with rapid increase of σ_N.

The question of the optimal lower photon energy and the optimal activity ratio has not been analysed further. It seems clear, however, that an evaluation of this should be related to the expected variation of subject thickness.

Base line errors. When calculating σ_A, the contribution of the end points will be weighted according to equation (11) by the factor $((n-2)/2)^2$. The position of the base line is thus critical for the precision of the method. In the four normal subjects, the manual positioning of the base line was partly governed by the widths of the vertebra and radiation beam. The points situated outside the end points were also taken into consideration, however, so that the end points should be in agreement with a reasonable extrapolation of these. The practical precision of the end points is therefore probably sometimes better than the theoretical precision, which may explain why the normal subject ML has a total precision s_A which is less than $\sigma_{A,\,mean}$ (Table 3). This phenomenon is even more marked in Table 4 concerning the series of measurements of aluminium, in which four out of five demonstrate lower s_A. In phantom measurements, however, the measuring conditions are so idealized that all points outside the object can often be approximated by a straight line, which will then

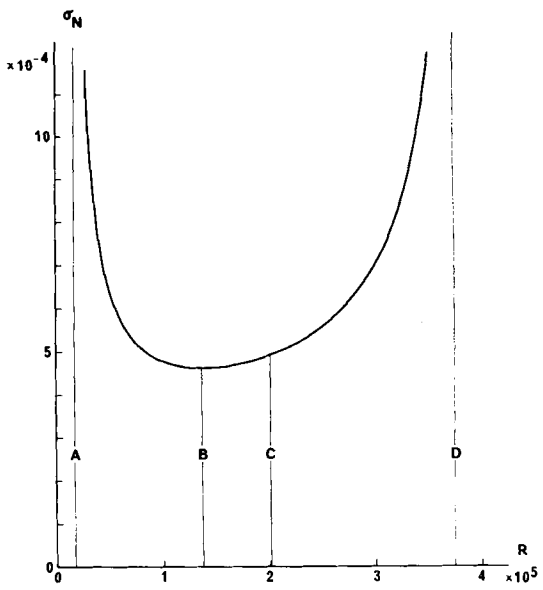

Fig. 4. σ_N as a function of number of counts R in the ^{241}Am channel under the condition $R + R' = 374645$ (measuring point x_{10} in Table 1). A and D are asymptotes to the curve, B is the minimum and C is the particular measuring point.

coincide with the base line. The reliability of the base line is in this case considerably greater than is suggested by equation (11).

There are possibilities, without changing the total investigation time, of reducing the errors due to the end points by: (1) eliminating unnecessary measuring points at the beginning and end of the measuring path, (2) increasing the measuring time or density of points in the end point region itself, and (3) possibly reducing the measuring time at the intermediate points $(x_2 - x_{n-1})$.

These measures, however, necessitate considerable modifications of the present procedure and probably also require a minicomputer for direct read-out of the N diagram.

Normal cases. With regard to the four normal cases (Table 3), it should be observed that s_A is the estimation of the standard deviation in an individual measurement. s_A varies within the range of 3.4 to 5.7 per cent (expressed as the coefficient of variation). The difference between s_A and $\sigma_{A,\,mean}$ may be regarded as a (probably low) estimate of the previously mentioned subject variations. For the normal subjects ML and SS the subject variations were small while the other two normal subjects showed greater differences between s_A and $\sigma_{A,mean}$. One reason for this may be movement of the subject during the measurement, which can be counteracted by a suitable fixation device. The four normal subjects were measured without any arrangements for fixation. It may be concluded from this limited test material that the short-term reproducibility is in the range of 3.4 to 5.7 per cent and with improved technique these values may probably be improved to 3 to 4 per cent.

DALÉN (1973) reports a precision with an X-ray spectrophotometric method of 1.9 per cent theoretically and 10 per cent experimentally in measuring of the third lumbar vertebra. The latter value was, however, improved to 2.7 per cent when the base line was adjusted manually. JUDY et coll. (1972) used a similar scanning method with ^{153}Gd (44 keV and 100 keV) as a dichromatic radiation source. They state the total precision to be 5 to 7 per cent for in vivo measurements of L3. The greatest source of error is considered to be the variation in determining the position of the base line.

Long-term control with aluminium. The results in Table 4 reveal that the total precision, s_A, is better than the theoretical precision, $\sigma_{A,mean}$ (except for Al 1 in June 1972). This fact may be explained on the basis of the discussion above concerning the influence of end points.

The change in A_{mean} for disc Al 1 from June 1972 to January 1974 is not significant at the 95 per cent level, calculated on the total precision, while, theoretically the change is significant at this level. During 1973 exchange of the detector took place and extensive service was performed on the electronic equipment. Bearing this in mind, the change of A_{mean} (2.2 %) must be considered small, suggesting a good working precision. Concerning the measurements of Al 2 there is no significant change from January to June 1974.

Acknowledgement

This investigation has received financial support from the Swedish Medical Research Council.

SUMMARY

Bone mineral content in lumbar vertebrae is determined by the attenuation of 59.6 keV (^{241}Am) and 662 keV (^{137}Cs) photons using the intermittent scanning technique. The precision, mainly influenced by decay variations, is analyzed mathematically. The reproducibility in patient measurements is also affected by variations in positioning, movements during measurement and base line errors. In four normal subjects the reproducibility ranged from 3.4 to 5.7 %. The long-term stability was better than 1 % during a five-month period as tested by phantom measurements.

ZUSAMMENFASSUNG

Der knöcherne Mineralgehalt der lumbalen Wirbel wurde durch die Dampfung von 59,6 keV (^{241}Am) und 662 keV (^{137}Cs) Photonen under Verwendung der intermittenten Skanning Technik bestimmt. Die Genauigkeit, hauptsächlich durch Schwankungen des Zerfalls beeinflusst, wurde mathematisch analysiert. Die Reproduzierbarkeit bei Patienten wird auch durch Veränderungen der Lage, Bewegungen während der Messung und Fehler in der Grundlinie beeinflusst. Bei vier normalen Personen schwankte die Reproduzierbarkeit zwischen 3,4 und 5,7 %. Die Langzeit Stabilität war während einer fünf-monatigen Testperiode mit Phantommessungen besser als 1 %.

RÉSUMÉ

Le contenu minéral osseux des vertèbres lombaires est mesuré par l'atténuation de photons de 59,6 keV (^{241}Am) et de 662 keV (^{137}Cs) en utilisant la technique de balayage intermittent. L'auteur analyse mathématiquement la précision de cette méthode qui dépend principalement des variations de décroissance. La reproductibilité des mesures sur les malades dépend aussi des différences de mise en place des malades, des mouvements au cours des mesures et des erreurs sur la ligne de base. Chez 4 malades normaux, la reproductibilité a varié de 3,4 à 5,7%. La stabilité à long terme est meilleure que 1% au cours d'une période de 5 mois d'après des tests de mesure faits sur fantôme.

REFERENCES

DALÉN N.: Bone mineral assay. Measuring sites; clinical applications. Thesis. Department of Medical Engineering, Karolinska Institutet, Stockholm 1973.

JUDY P. F., CAMERON J. R., JONES K. M. and ORT M. G.: Determination of vertebral bone mineral mass by transmission measurements. USAEC Progress Report COO-1442-126 (1972).

ROOS B.: Bestämning av mineralinnehåll i lumbalkotor genom mätning av transmitterad gammastrålning från två radioaktiva nuklider. (In Swedish.) Radiofysiska institutionen, Göteborgs universitet, Gothenburg 1970.

— and SKÖLDBORN H.: Dual photon absorptiometry in lumbar vertebrae. I. Theory and method. Acta radiol. Ther. Phys. Biol. 13 (1974), 266.

— ROSENGREN B. and SKÖLDBORN H.: Determination of bone mineral content in lumbar vertebrae by a double gamma-ray technique. Bone Measurement Conference, Chicago, Ill. (1970), Proc. CONF-700515, p. 243.

WOOTEN W. W.: Bone densitometry. The two photon technique and fat content of the bone. Thesis. University of California, Los Angeles 1971.